

PIPE COOLING OF SUPERCONDUCTING CAVITIES

A. Chincarini[§], R. Ballantini, G. Gemme, R. Parodi, *INFN, Genova, Italy*

Abstract

Cryostat and cryogenic system account for a relevant amount of the total SRF accelerator budget. Pipe cooling, if proven successful, will greatly simplify the cryogenic design of an accelerator and, possibly, substantially reduce the construction and operation costs.

We explore the RF characteristics of pipe cooled superconducting cavities versus bath cooled ones, using different pipe configurations and different LHe temperatures. Typical applications and fits with experimental data will be shown, and the limits of the cooling method will be discussed.

INTRODUCTION

Superconducting RF cavities have been used in particle accelerators for several decades, these cavities being traditionally operated immersed in a liquid helium bath. Nevertheless, several attempts have been made to make use of the numerous operational and cost advantages of pipe cooling configuration: reduction in liquid helium inventory, minimized cooldown/warmup times and elimination of the LHe vessel, which reduces the sensitivity to microphonics and provides easier access to all cavity components [1].

Focusing on structures with cylindrical symmetry, we compare the expected performances of bath cooled and pipe cooled single cells, in terms of reduction in Q_0 values and peak surface fields. A section is dedicated to the comparison with experimental data coming from bath cooled cavities, where the losses were due to effects other than thermal (e.g. electron emission, multipacting, etc.).

MODEL

We approach the cavity thermal modelling in two steps: first we consider a purely thermal problem, with no other dissipation mechanisms, and compare the efficiency of different pipe configurations and LHe temperatures; then we take real measurements of the averaged surface resistance $\langle R_{surf} \rangle$ versus E_{acc} in bath cooled cavity and use this curve to extrapolate the $\langle R_{surf} \rangle$ in the case of pipe cooling.

Surface resistance

When considering purely Ohmic dissipations, our calculations are based on an analytical model for the BCS resistance R_{BCS} (Wilson formula), which has been proven to adequately match both the experimental data and the theoretical calculations [2, 3]. A small phenomenological residual resistance R_{res} , typically of the order of 10 – 50 n Ω , is then added.

R_{BCS} and R_{res} are only adequate to look at the cavity from a purely Ohmic point of view, that is to study the cavity behaviour in the hypothesis that the only limiting factors are the BCS surface resistance, the thermal conductivity of the material and the way the cavity is cooled on the external surface.

Considering experimental data though, one sees that the cavity performances are often limited by other processes (like field emission, multipacting or surface defects) much earlier than the predicted limit given by the theoretical R_{BCS} [4]. Since our aim is to look for applicability of pipe cooling and not to justify experimental curves, we can take the measured average surface resistance $\langle R_s \rangle$ curves for a bath cooled cavity as *given effective residual resistance*, that is:

$$R_s(\vec{r}, T_{int}, f, B_{surf}) = \tilde{R}_{res}(E_{acc}) + R_{BCS}(T) \quad (1)$$

where $\tilde{R}_{res}(E_{acc})$ is a suitable function that fits the experimental data. For the cases we have considered, the main contribution to the $\langle R_s \rangle$ came from field emission phenomena. It was therefore possible to use reasonable analytical functions to fit the measurements:

$$\tilde{R}_{res} = R_{res} + \lambda_1 E_{acc} + \lambda_2 E_{acc} (\lambda_3 E_{acc})^{5/2} \cdot e^{\left(-\frac{\lambda_4}{\lambda_3 E_{acc}} \right)} \quad (2)$$

where $R_{res} = \lim_{E_{acc} \rightarrow 0} \langle R_s \rangle$ and λ_i are free dimensional parameters.

The term multiplying λ_1 takes into account the linear trend observed in sputtered Nb on Cu cavities at low fields [5] while the term multiplying λ_2 is the Fowler-Nordheim term [4]. Once the λ_i are found through a fit, eq. (1) and (2) are used in the thermal calculation for a bath cooled cavity and the results are checked to verify that they match the experimental data again. It is then straightforward to modify the external condition to account for pipe cooling.

Thermal conductivity

The thermal conductivities used in the calculation come from experimental data [6], linearly interpolated and properly scaled for the RRR values when needed. The different values of the thermal conductivity λ used in the simulations have been computed scaling the measured curve (RRR=60) according to the Wiedmann-Franz [7] law:

$$\lambda(\text{newRRR}) = \lambda(\text{RRR} = 60) \frac{\text{newRRR}}{60}$$

[§]andrea.chincarini@ge.infn.it

For Nb on Cu sputtered cavities, only Cu has been considered to account for heat transport, thus neglecting the sputtered Nb layer.

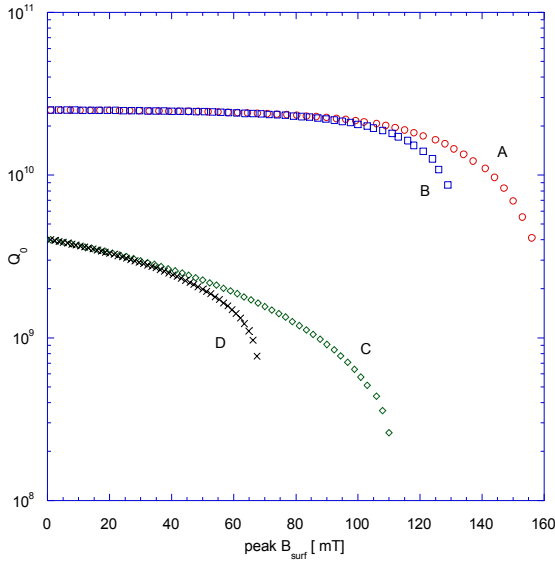


FIG. 1. Performance comparison computed for a TRASCO $\beta=0.85$ cavity. Simulation parameters are: $f = 343$ MHz, $G = 250 \Omega$, $R_{\text{res}} = 10$ n Ω , Cu thickness = 6 mm, RRR = 275. ‘A’ and ‘B’ are respectively bath and pipe cooled @ $T_{\text{LHe}} = 1.8$ K, ‘C’ and ‘D’ are bath and pipe cooled @ $T_{\text{LHe}} = 4.2$ K.

Metal – LHe interface

Across the interface between a solid and LHe there exists a temperature jump $\Delta T = T_s - T_B$, where T_s is the solid outer surface temperature and T_B is the bath temperature (both in K). ΔT is related to the heat flux q_e in Wm^{-2} across the interface so that T_s can be described by the following relation [8]:

$$T_s = \begin{cases} \left(T_B^4 + 4q_e R_k T_B^3 \right)^{1/4} & T_B \leq 2.18\text{K} \\ T_B + \left(\frac{q_e}{h} \right)^{1/4} & 2.18 < T_B \leq 4.2\text{K} \end{cases} \quad (3)$$

This expression shows that ΔT is also dependent on the LHe regime: for superfluid LHe ($T_B \leq 2.18\text{K}$), T_s is driven by the Kapitza resistance R_k , whose values differs substantially depending on the surface chemical treatment [9]. In our calculation we have used more conservative numbers [10], although we have checked that the results using more favorable values are qualitatively the same.

For the LHe-I regime, T_s is proportional to a power of q_e , whose parameters have been experimentally determined to be $h \approx 1.23 \cdot 10^4$ and $a \approx 1.45$ [11]. Equation (3) holds below a critical heat flux ($\approx 10^4 \text{Wm}^{-2}$) at which film boiling sets on and the heat transfer rate sharply decreases by approximately one order of magnitude.

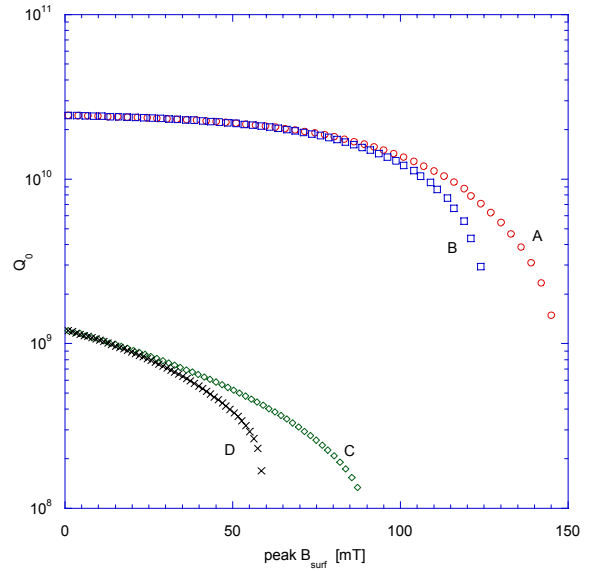


FIG. 2. Performance comparison computed for a TRASCO 700 MHz cavity. Simulation parameters are: $f = 707$ MHz, $G = 250 \Omega$, $R_{\text{res}} = 10$ n Ω , Cu thickness = 4 mm, RRR = 275. ‘A’ and ‘B’ are respectively bath and pipe cooled @ $T_{\text{LHe}} = 1.8$ K, ‘C’ and ‘D’ are bath and pipe cooled @ $T_{\text{LHe}} = 4.2$ K.

RESULTS

Thermal effects

This simulation set compares the expected results for a bath cooled versus a pipe-cooled cavity, when only BCS surface resistance and the material thermal conductivity are taken into account.

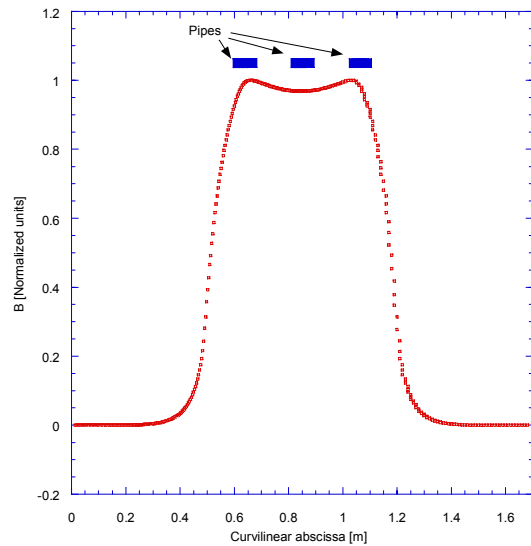


FIG. 3. Pipes position relative to the magnitude of the magnetic field on the surface. Each pipe has a diameter of approximately 6 cm.

FIG. 1 and FIG. 2 show respectively the results for a TRASCO $\beta = 0.85$ Nb-Cu cavity and for a TRASCO 700 MHz Nb bulk cavity, both operated on the TM_{010} [12, 13, 14]. As expected, the maximum B_{surf} predicted for bath cooling is much higher than the experimental values, thanks to the lack of other dissipation mechanisms. The pipe scheme used for one of these simulations are sketched in FIG. 3, where the pipes position is plotted versus the curvilinear abscissa running on the cavity's profile. The normalized B profile pictured in FIG. 3 refers to the TRASCO $\beta = 0.85$ cavity. For this test, only three pipes of approximately 6 cm in diameter are used to cool the cavity, and they have been positioned in the highest B field region yielding a cavity surface coverage of approximately 17%.

The simulations done by playing with different pipe numbers (maintaining the same surface coverage) and cavity wall thickness show that there is a non-negligible freedom in choosing the pipe distribution, provided enough surface coverage exists in the high field region. The simulations discussed above however, do not include surface defects.

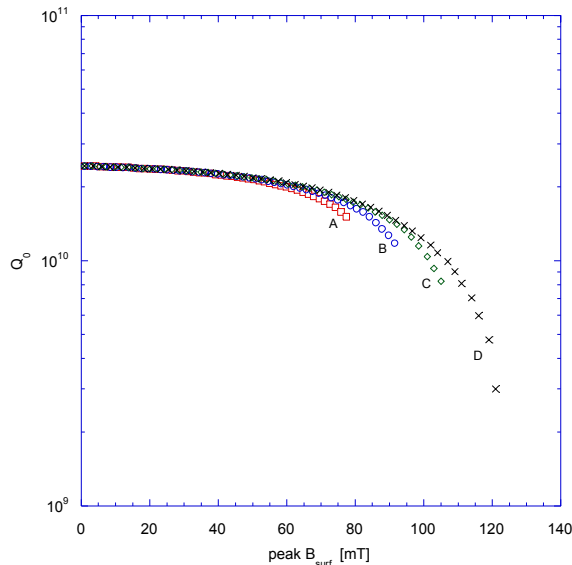


FIG. 4. Performances of a three-pipes cooled, 700 MHz single cell, with different Nb purity. Curve 'A' is for a RRR=50, 'B' for a RRR=100, 'C' RRR=250, 'D' RRR=500.

Frequency and RRR dependence

Pipe cooling efficiency can also be tested as function of several cavity parameters. We have run some simulations to study the thermal behavior dependence on the cavity's frequency and the Nb RRR.

FIG. 4 shows the Q_0 performances with several RRR values and refers to a TRASCO 700 MHz cavity cooled at $T_{LHe} = 1.8$ K with the help of three pipes of diameter $\varnothing = 2.2$ cm, for a surface coverage of $\approx 23\%$. FIG. 4 confirms the need for a high thermal conductivity (RRR>200) and

shows that extreme values do not appreciably increase the stability.

Frequency dependence has been tested by scaling the linear dimensions of a 700 MHz cavity in order to have its resonant frequency going from 500 MHz up to 3 GHz, all cavities cooled at $T_{LHe} = 1.8$ K.

It is important to note that we have scaled the cavity linear dimensions and tube diameters (in order to keep the surface coverage a constant), whereas the wall thickness has been kept unchanged (2 mm). All other parameters such as residual resistance, geometry factor and LHe temperature have been kept constant throughout all computations.

We have simulated the cooling using 3 pipes, whose diameters ranged from 3.1 cm (for the 500 MHz cavity) to 5 mm (3 GHz cavity), keeping the surface coverage at 24%. FIG. 5 shows the Q_0 performances for the cavity scaled to operate at 500 MHz and 3 GHz. These results are obviously valid for a very ideal situation, especially regarding the cavity surface loss mechanism.

Furthermore, keeping the thickness of the cavity as a constant over the whole frequency range, for example, would pose serious mechanical problems at low frequency. Similarly, scaling the pipe diameters to 5 mm may be unpractical.

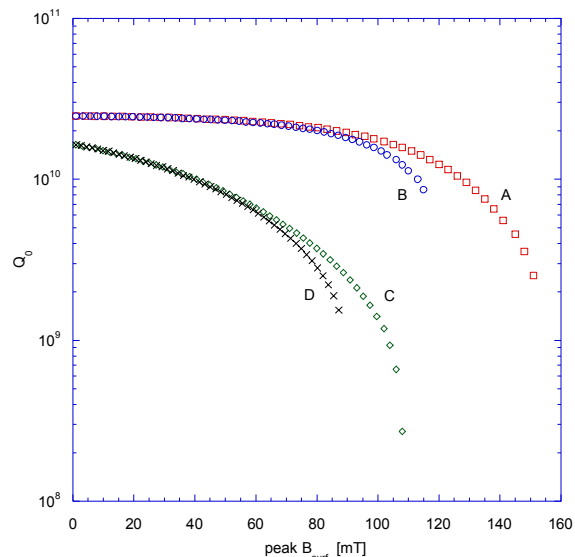


FIG. 5. Performance comparison for a 2 mm thick, bulk Nb cavity whose dimensions were scaled to operate at 500 MHz and 3 GHz. RRR = 300 for all curves. Curve 'A': bath cooled, 500 MHz; 'B': pipe cooled, 500 MHz; 'C': bath cooled, 3 GHz; 'D': pipe cooled, 3 GHz.

Surface defects

In our code the surface defect can only be simulated by changing the properties of an annular surface, whose typical dimensions are 40 mm in radius and 1 mm in height. We acknowledge that this is a very crude representation of a surface defect, it is nevertheless

instructive to look at the relative performances of a pipe-cooled cavity when in presence of such a bad area.

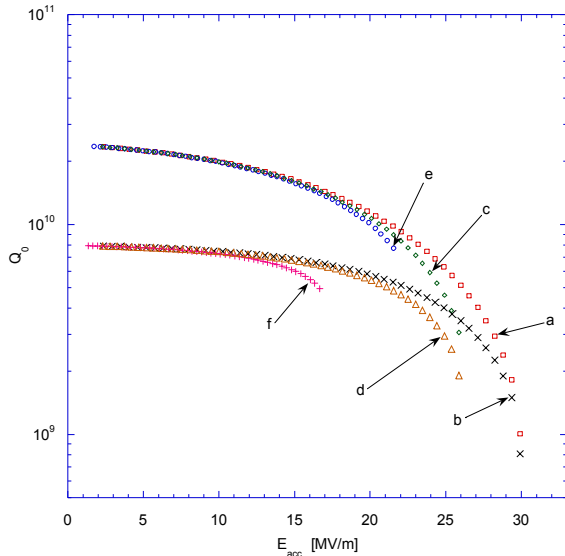


FIG. 6. Surface defect simulation for a 1500 MHz cavity. Curves are labeled as follows: ‘a’ bath cooled, no surf. defect; ‘b’ bath cooled with surf. defect; ‘c’ five pipes $\varnothing \approx 2$ cm, surf. coverage 38%, no defect; ‘d’ same as ‘c’ but with surf. defect; ‘e’ single pipe $\varnothing \approx 7.1$ cm, surface coverage 38%, no defect; ‘f’ single pipe with surf. defect.

The simulation, whose results are plotted in FIG. 6, shows that in the bath cooled case the presence of the defect does not deteriorate the achievable peak surface fields (curves ‘a’ and ‘b’ in FIG. 6). This means that the cavity may perform very well in the bath and yet may turn out to be strongly affected by the defect when pipe cooled (curves ‘b’ and ‘f’). The surface defect though, is not the only responsible for the cavity behavior. A wiser choice for the pipes distribution could help, that is, a greater number of pipes suitably distributed perform better than a lesser number, even if the latter surface coverage is comparable to the multi-pipe configuration.

A configuration involving several pipes is therefore more forgiving in case of a surface bad spot (compare curves ‘d’, ‘f’ and ‘c’ in FIG. 6).

For a better understanding of the performances in presence of a surface defect, we have run a Monte Carlo simulation involving a randomized defect position and dimension both for a bath cooled cavity and for 2 different pipe schemes (3 and 5 pipe configuration with the same surface coverage). The results are plotted in FIG. 7, where the average Q_0 versus average maximum field are plotted, together with the convex hull that encompass all the Monte Carlo runs. The “3 pipes” area (green) in FIG. 7 is roughly 4 times greater than the “bath” area (blue), whereas the “5 pipes” area (red) is approx. 3 times greater than the “bath” area. The area sizes and positions once more underline that a pipe-cooled

cavity may suffer from a greater variability in performance, when in presence of a surface defect.

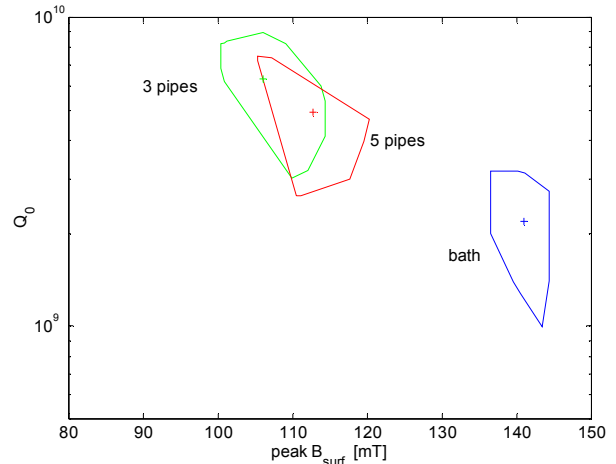


FIG. 7. Monte Carlo simulation of a 700 MHz cavity with a sizeable, random surface defect. The areas represent the locus of the points (B, Q_0) with maximum performance. The “+” are the average on the Monte Carlo runs.

MEASUREMENT FITS.

Real cavities performance curves often exhibit signatures of effects like electron field emission and multipacting. Because of their variability in strength and occurrence, it is difficult to account for them in a model.

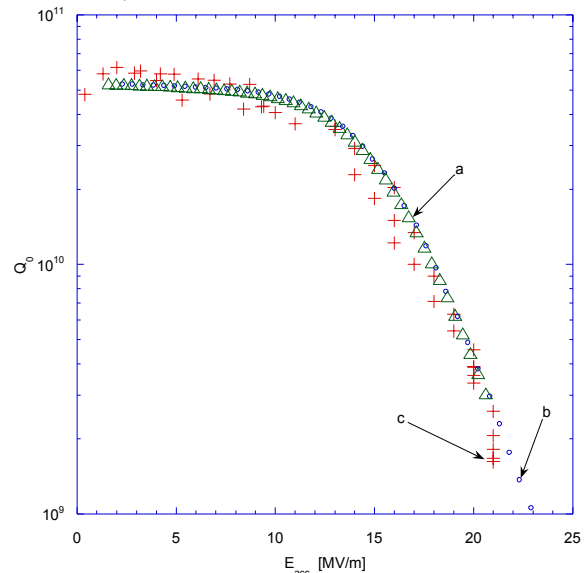


FIG. 8. Performance simulation and experimental data for a 700 MHz cavity suffering from electron field emission. ‘a’ (Δ) pipe cooled simulation; ‘b’ (\circ) bath cooled simulation; ‘c’ ($+$) measured data.

In this paper we have considered a set of measurement on a TRASCO 700 MHz and TRASCO 347.2 MHz cavity performed at Saclay, France [15]. These measurements clearly show a Q_0 value degradation due to field emission,

therefore we have used eq. (1) and (2) to fit the effective residual resistance, where the Fowler-Nordheim term accounts for the sharp increase of $\langle R_s \rangle$ at relatively low accelerating fields.

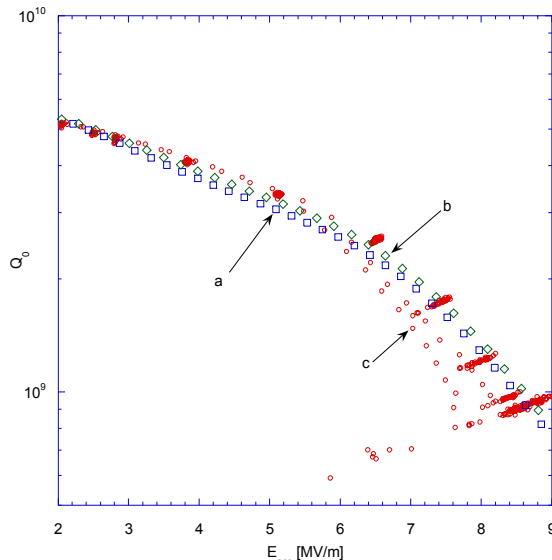


FIG. 9. Performance simulation and experimental data for a 347 MHz cavity @ 4.2 K, suffering from electron field emission. ‘a’ pipe cooled simulation; ‘b’ bath cooled simulation; ‘c’ measured data.

FIG. 8 and FIG. 9 show the measured data, the simulation for the bath cooled cavity and the expected performance of the pipe cooling configuration on the same plot. For the 700 MHz cavity, we have simulated three pipes of approximately 1.5 cm in diameter equally spaced around the maximum value of the surface magnetic field.

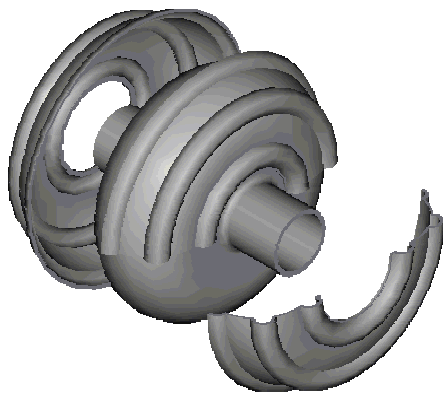


FIG. 10. Proposed method for adding pipes to the cell.

If we restrict our analysis to relatively low E_{acc} values, pipe cooling does not have any appreciable effect. The difference lies in the abrupt transition that takes place at a far lower field than the expected bath cooled counterpart.

The simulations we performed, compared to the available real data on cavities limited by field emission, show that pipe cooling should not alter the overall cavity performance.

Electron emission normally occurs at field’s values far lower than the one needed for thermal breakdown. It is therefore reasonable that, for those field values, pipe cooling should perform nearly as well as bath cooling.

In order to validate our code and support the method with more measures, we are planning to use a well characterized 3 GHz cavity. We will add pipes to it by forming a Nb shell with the same cavity profile, but already shaped with the pipes. The shell will be electron-beam welded onto the cavity so that the whole assembly can be connected to the LHe piping (see FIG. 10).

CONCLUSION

Bulk niobium and Nb-Cu technologies are nowadays quite mature. We can therefore envisage an improvement in terms of design freedom and cost management for pipe cooled structures.

The remark that real pipe cooled cavities are much more sensitive to any non-ideality, due to their lessened heat dissipation capabilities, is generally true. Nevertheless, the cavity behavior can be tamed by properly choosing the pipes size and distribution.

On the basis of our work, we have started a project in order to check the validity and the limits of the pipe cooling system for a 3 GHz cavity set.

REFERENCES

- [1] J. Susta, P. Kneisel and M. Wiseman, Proceedings of the International Conference on Particle Accelerator, 1993, edited by IEEE, p. 1060.
- [2] P. B. Wilson, SLAC laboratory report, SLAC-TN-70-35 (1970).
- [3] A. Chincarini, G. Gemme, R. Ballantini and R. Parodi, Physical Review ST Accelerator and Beams **6**, 083201, (2003).
- [4] H. Padamsee, J. Knobloch and T. Hays, Rf Superconductivity for Accelerators (John Wiley&sons Inc, 1998).
- [5] C. Benvenuti, S. Calatroni *et al.*, Physica C **316**, 153-188, (1999).
- [6] NBS monograph.
- [7] M. W. Zemansky, Heat and Thermodynamics, (McGraw - Hill, 1968), p. 94.
- [8] P. Fernandes, R. Parodi, Cryogenics **11**, 433, (1984).
- [9] A. Boucheffa and M.X. Francois, Proceedings of the Seventh Workshop on RF Superconductivity, 1995, pp. 659-669.
- [10] K. Mittag, Cryogenics **13**, 94, (1973).

- [11] C. Johannes, Proceedings of the International Conference on Cryogenic Engineering, ICEC 3, p. 97, (1970).
- [12] <http://trasco.lnl.infn.it/>
- [13] D. Barni, Proceedings of the International Conference on RF Superconductivity, 2001, Tsukuba (JP), proc. ref. TA009.
- [14] R. Parodi, Proceedings of the International Conference on RF Superconductivity, 2001, Tsukuba (JP), proc. ref. PR005.
- [15] H. Safa, Proceedings of the International Conference on RF Superconductivity, 2001, Tsukuba (JP), proc. ref. MA008.